Available online at www.sciencedirect.com
ScienceDirect
Polymer 47 (2006) 7001–7012
polymer
www.elsevier.com/locate/polymer

Synthesis and electroluminescence properties of a novel tetraphenylsilane–oxadiazole–diphenyl(*para*-tolyl)amine polymer

Rong-Ho Lee [a,*], Hsin-Fang Hsu [a], Li-Hsin Chan [b], Chin-Ti Chen [b]

[a] *Department of Chemical Engineering, National Yunlin University of Science & Technology, Yunlin 640, Taiwan, ROC*
[b] *Institute of Chemistry, Academia Sinica, Taipei 11529, Taiwan, ROC*

Received 5 March 2006; received in revised form 11 July 2006; accepted 31 July 2006
Available online 22 August 2006

Abstract

A novel triarylaminooxadiazole-containing tetraphenylsilane light-emitting polymer (PTOA) has been synthesized. Excellent thermal stability was observed due to the presence of a rigid tetraphenylsilane-based polymer backbone ($T_g = 218$ °C, $T_d = 373$ °C). In solution, PTOA shows photoluminescence (PL) with an emission maximum at 426 nm, which is attributed to the light-emitting unit of the triarylaminooxadiazole group. In solid film, the emission maximum of PL is observed at 458 nm, a 32 nm red-shift from the PL in solution. The solvatochromic effect and excimer formed in the solid film are responsible for the red-shifting and broadening of the PL emission band. The PL stability and morphology of the PTOA solid film were further investigated by thermal annealing at elevated temperatures. No significant difference in the PL spectra or morphology was observed between a pristine sample and a repeatedly thermally annealed film (at 200 °C). PTOA-based PLED shows EL with a main peak at 458 nm accompanied by a shoulder at around 530 nm. The light emission from electromer or electroplex leads to a broadening of the EL spectra (400–650 nm), which corresponds to the interaction between the oxadiazole and diphenyl(4-tolyl)amine groups in different polymer segments or chains. A sky blue emission (Commission Internationale de L'Eclairage ($CIE_{x,y}$) coordinates (0.20,0.23)) was obtained for PTOA-based PLED. The brightness and efficiency of the PLED can be as high as 248 cd/m^2 and 0.54 cd/A, respectively. The EL of PTOA-based PLED has been further improved by blending the PTOA with poly(*n*-vinylcarbazole) (PVK) in different concentrations. The effects of concentration on the PL and EL were studied for the PTOA–PVK composite film-based PLEDs.

Keywords: Tetraphenylsilane; Oxadiazole; Polymer light-emitting device

1. Introduction

Recently polymer light-emitting displays (PLEDs) have been studied extensively and appeared ready for commercialization in the flat-panel display market due to its low turn on voltage, high brightness, high efficiency, easy processing, and low cost fabrication [1,2]. In addition to the processing parameters and device configuration, the electroluminescence (EL) properties of PLEDs are predominantly determined by the intrinsic character of the light-emitting polymer (LEP), such as photoluminescence (PL), thermal stability, film formability, and chain morphology [3,4]. The development of LEPs with excellent electroluminescence properties is an important issue for the application of LEPs in the flat-panel display.

In order to obtain a PLED with high brightness and high efficiency, the charge transport and balance throughout the light-emitting layer must be considered [5,6]. The charge transport and balance are dependent on the chemical structure and functional groups of the LEP. For example, oxadiazole containing compounds with electron-drawing properties have been used as the electron-transporting layer for organic light-emitting devices (OLEDs) [7]. The oxadiazole group was usually grafted onto or incorporated into the polymer backbone of the blue LEP, as with the poly(phenylene vinylene) and polyalkylfluorene materials [8–13]. In addition to the improvement in the electron-transporting capability, the introduction of the oxadiazole group could enhance the electron affinity of the blue LEP, which leads to a reduction in

* Corresponding author. Tel.: +886 5 5342601x4625; fax: +886 5 5312071.
E-mail address: lerongho@yuntech.edu.tw (R.-H. Lee).

0032-3861/$ - see front matter © 2006 Elsevier Ltd. All rights reserved.
doi:10.1016/j.polymer.2006.07.074

the energy barrier between the light-emitting layer and metal cathode [8–13]. Furthermore, the oxadiazole derivatives are known to be the blue emitters in OLEDs and PLEDs [14–16]. Oxadiazole containing small molecular light-emitting materials with excellent electroluminescence properties has been reported [17–20]. In addition, the aromatic amine group has usually been grafted onto or incorporated into the polymer backbone to enhance the hole-transporting properties of LEP [21,22]. The bipolar characteristics of LEP containing electron- and hole-transporting moieties are essential for the carrier transport and balance throughout the light-emitting layer. This is helpful in the enhancement of the brightness and efficiency of PLEDs [23–27].

In addition to the brightness and efficiency, the thermal stability and photoluminescence (PL) or electroluminescence (EL) spectral stability also play important roles in the display application of LEP. The operational lifetime of a PLED is directly related to the T_g and the thermal stability of the LEP [28]. Bulky substituents and rigid groups are usually grafted onto or incorporated into the polymer backbone to obtain LEPs with excellent thermal stability, such as the dendron, triphenylamine, tetraphenyl-phenylenediamine, and tetraphenylsilane groups [29–32]. Besides the excellent thermal stability, the tetraphenylsilane-containing compounds, either as small molecules or polymers, have been proven to be effective as blue light-emitting materials in the fabrication of high brightness blue OLEDs [17–20,32,33]. In addition, the aggregation due to π–π stacking sometimes results in the formation of an excimer between the polymer segments or chains, which leads to the broadening and quenching of the PL or EL of PLEDs [34–38]. This is a critical issue for the application of LEP in displays. The aggregation and excimer effect could be suppressed by the incorporation of bulky and branched side chain substituents into the polymer backbone, or blending the LEP with other conjugated polymers [39–44].

Accordingly triarylaminooxadiazole-containing tetraphenylsilane light-emitting polymer (PTOA) has been designed and synthesized. Deep blue emission is expected for PTOA-based PLEDs. Furthermore, high thermal stability is also expected for the PTOA with a rigid tetraphenylsilane group in the polymer backbone. The thermal and PL properties of PTOA have been characterized. The correlation between the polymer film morphology and PL stability was also investigated. The EL properties of the PTOA-based PLED at various applied voltages are also discussed. In order to reduce the aggregation and excimer effect between the polymer chains the PTOA was blended with poly(*n*-vinylcarbazole) (PVK) in different concentrations. The concentration effect on the PL and EL has been studied for the PTOA–PVK composite film-based PLEDs.

2. Experimental section

2.1. Synthesis of LEP

All reactions and manipulations were performed in a nitrogen atmosphere using standard Schlenk techniques. All chromatographic separations were carried out on silica gel. *O*-Xylene, diethyl ether, and anisole were distilled over sodium/benzophenone in a nitrogen atmosphere. Dimethylformamide (DMF) was dried over $CaSO_4$. Chemicals were reagent grade and purchased from Aldrich, Fluka, Sigma, and RDH Chemical Co. All chemicals were used as-received unless otherwise described. Schemes 1–3 illustrate the synthetic route for the preparation of the triarylaminooxadiazole-containing tetraphenylsilane light-emitting polymer. The detail of synthesis procedures is reported as follows:

2.1.1. (4-Methylphenyl)diphenylamine (compound *1*)

(4-Methylphenyl)diphenylamine was synthesized according to the Tosoho procedure [45,46]. The reaction mixture, containing diphenylamine (16.90 g), 4-bromotoluene (13.44 mL), NaO^tBu (11.53 g), $Pd(OAc)_2$ (0.0560 g), $P(t\text{-}Bu)_3$ (0.2467 mL), and *O*-xylene (125 mL), was reacted at 120 °C in a nitrogen atmosphere for 2 h. After reaction, the mixture was poured into water and extracted with dichloromethane. The organic layer was dried over anhydrous magnesium sulfate followed by evaporation of the solvent in a rotary evaporator. The crude product was purified by flash column chromatography (silica

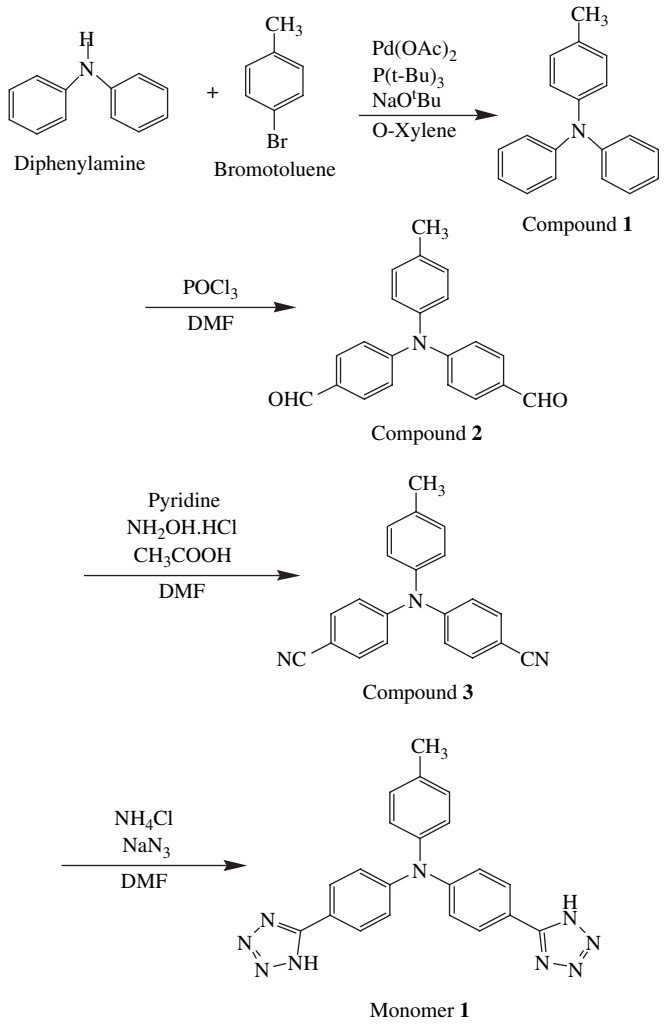

Scheme 1. Synthesis of monomer **1**.

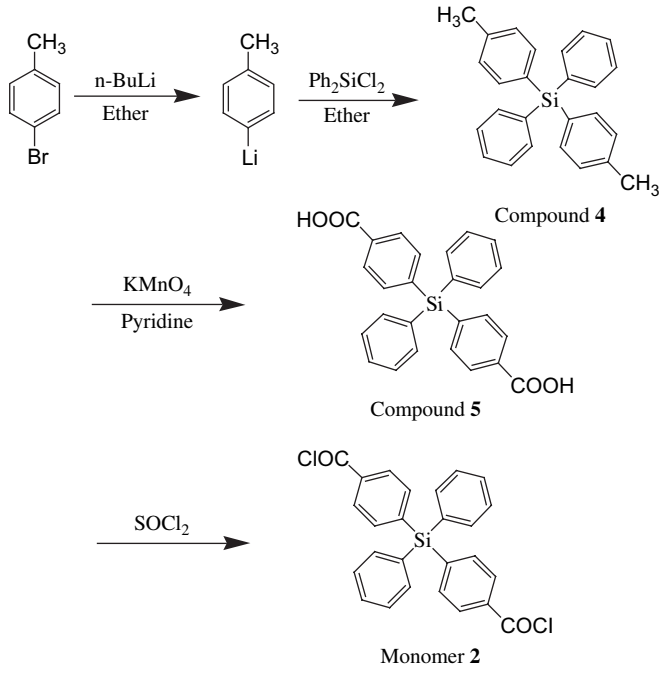

Scheme 2. Synthesis of monomer **2**.

gel, EA/hexane as eluent). The yield of the white solid product was 93.3% (24.19 g). ^{1}H NMR (400 MHz, $CDCl_3$) δ (ppm): 7.22–7.18 (m, 4H), 7.06–7.02 (m, 6H), 6.99–6.92 (m, 4H), 2.29 (s, 3H). Anal. Calcd for $C_{19}H_{17}N$: C, 88.18; H, 5.44; N, 5.31. Found: C, 87.91; H, 6.55; N, 5.40.

*2.1.2. (4,4′-Dialdehyde-4″-methyl)triphenylamine (compound **2**)*

Phosphorus oxychloride ($POCl_3$, 19.57 mL) was slowly added into the reaction mixture of compound **1** (5.1870 g) and dimethylformamide (41.496 mL) at 0 °C in a nitrogen atmosphere. After the solution became yellow the reaction mixture was then heated to 90 °C and reacted for 6 h. After cooling the reaction mixture was slowly poured onto crushed ice followed by neutralization with sodium carbonate solution. The solution was further extracted with ethyl acetate. The organic layer was dried over anhydrous magnesium sulfate followed by evaporation of the solvent in a rotary evaporator. The crude product was purified by flash column chromatography (silica gel, EA/hexane as eluent). The yield of the yellow-greenish solid product was 24.8% (3.2 g). ^{1}H NMR (400 MHz, $CDCl_3$) δ (ppm): 9.87 (s, 2H), 7.74 (d, 4H, $J = 8.7$ Hz), 7.18 (d, 2H, $J = 8.3$ Hz), 7.15 (d, 4H, $J = 8.6$ Hz), 7.04 (d, 2H, $J = 8.2$ Hz), 2.37 (s, 3H). Anal. Calcd for $C_{21}H_{17}NO_2$: C, 80.45; H, 5.64; N, 4.53. Found: C, 79.78; H, 5.43; N, 4.44.

*2.1.3. (4,4′-Cyano-4″-methyl)triphenylamine (compound **3**)*

A reaction mixture containing compound **2** (3.153 g), $NH_2OH{\cdot}HCl$ (1.66 g), CH_3COOH (3.93 mL), pyridine (2.41 mL), and DMF (7.30 mL) was stirred and reacted at 140 °C in a nitrogen atmosphere for 3 h. After cooling, water (250 mL) was slowly added into the reaction mixture followed by neutralization with sodium carbonate solution. The solution was further extracted with ethyl acetate. The organic layer was dried over anhydrous magnesium sulfate followed by evaporation of the solvent in a rotary evaporator. The crude product was purified by flash column chromatography (silica gel, EA/hexane as eluent). The yield of the orange solid product was 68.2% (2.1 g). ^{1}H NMR (400 MHz, $CDCl_3$) δ (ppm): 7.48 (d, 4H, $J = 8.9$ Hz), 7.18 (d, 2H, $J = 7.9$ Hz), 7.07 (d, 4H, $J = 8.8$), 7.00 (d, 2H, $J = 8.3$), 2.36 (s, 3H). Anal. Calcd for $C_{21}H_{15}N_3$: C, 82.17; H, 4.49; N, 13.12. Found: C, 81.46; H, 4.85; N, 13.58.

*2.1.4. (4,4′-Tetrazolyl-4″-methyl)triphenylamine (monomer **1**)*

A reaction mixture containing compound **3** (0.6 g), NaN_3 (4.17 g), NH_4Cl (3.4296 g), and DMF (15.44 mL) was

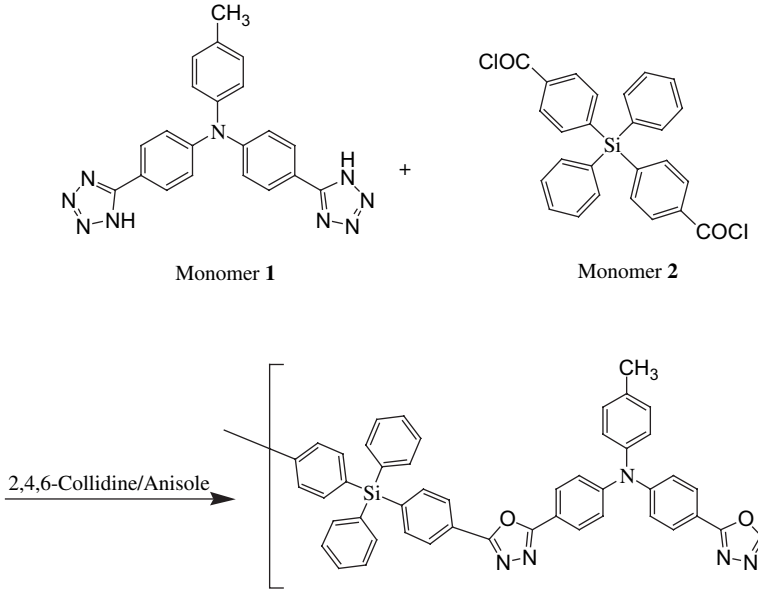

Scheme 3. Synthesis of light-emitting polymer.

heated to reflux and stirred in a nitrogen atmosphere for 75 h. After cooling to room temperature, the reaction mixture was slowly poured into crushed ice. The precipitate was filtered and dissolved in ethyl acetate. The organic layer was dried over anhydrous magnesium sulfate followed by evaporation of the solvent in a rotary evaporator. The product was further dried under vacuum. The yield of the white solid product was 40.8% (0.32 g). ^{1}H NMR (400 MHz, DMSO) δ (ppm): 7.93 (d, 4H, $J = 7.7$ Hz), 7.23 (d, 2H, $J = 6.6$ Hz), 7.17 (d, 4H, $J = 7.7$ Hz), 7.07 (d, 2H, $J = 7.1$ Hz), 2.31 (s, 3H). Absorption of two protons could not be observed for the two tetrazolyl groups. Anal. Calcd for $C_{21}H_{17}N_9$: C, 63.79; H, 4.47; N, 31.68. Found: C, 63.74; H, 4.58; N, 31.54.

2.1.5. (4,4′-Dimethylphenyl)diphenylsilane (compound **4**)

n-Butyllithium (100 mL) was added drop-wise to dry ether solution containing 4-bromotoluene (21.16 mL) at −20 °C in a nitrogen atmosphere, via syringe. The reaction mixture was reacted for 5 h. After the reaction mixture became colorless, the solution containing dichlorodiphenylsilane (15.14 mL) and dry ether (200 mL) was then added drop-wise to the reaction mixture via syringe. The reaction mixture was allowed to warm up to room temperature and reacted overnight. The reaction mixture was quenched with water (250 mL) and extracted with ether. The organic layer was dried over anhydrous magnesium sulfate followed by evaporation of the solvent in a rotary evaporator. A white solid crude product was purified by flash column chromatography (silica gel, EA/hexane as eluent). The yield of the white solid product was 88.8% (23.3 g). ^{1}H NMR (400 MHz, $CDCl_3$) δ (ppm): 7.53 (t, 4H, $J = 7.8$ Hz), 7.43 (d, 4H, $J = 7.8$ Hz), 7.38 (t, 2H, $J = 7.0$ Hz), 7.34 (d, 4H, $J = 7.4$ Hz), 7.17 (d, 4H, $J = 7.8$ Hz), 2.35 (s, 6H). Anal. Calcd for $C_{26}H_{24}Si$: C, 85.81; H, 6.43. Found: C, 85.58; H, 6.58.

2.1.6. (4,4′-Dicarboxyphenyl)diphenylsilane (compound **5**)

A solution containing (4,4′-dimethylphenyl)diphenylsilane (1.092 g), $KMnO_4$ (9.48 g), H_2O (20 mL), and pyridine (60 mL) was heated to reflux and reacted overnight in a nitrogen atmosphere. After cooling to room temperature, the reaction was quenched with methanol (250 mL). The MnO_2 in the reaction mixture was removed by filtration and washed with 500 mL of hot water. After cooling, hydrogen chloride was added to the reaction solution until the pH value achieved one. The white solid crude product was then precipitated from the solution. The crude product was collected by filtration and washed with 1000 mL of deionized water. The residue of compound **4** in the crude product was dissolved and removed with hexane. The final product was dried under vacuum. The yield of the white solid product was 97.9% (1.24 g). ^{1}H NMR (400 MHz, $CDCl_3$) δ (ppm): 12.35 (s, 2H), 8.06 (d, 4H, $J = 19.5$ Hz), 7.67(d, 4H, $J = 7.3$ Hz), 7.53 (t, 4H, $J = 6.2$ Hz), 7.46–7.39 (m, 6H). Anal. Calcd for $C_{26}H_{20}O_4Si$: C, 73.36; H, 4.73. Found: C, 73.49; H, 4.71.

2.1.7. (4,4′-Dichlorocarbonylphenyl)diphenylsilane (monomer **2**)

A reaction mixture containing compound **5** (0.849 g) and thionyl chloride ($SOCl_2$, 10 mL) was heated to reflux in a nitrogen atmosphere overnight. After cooling, all volatile liquid was removed under reduced pressure of the reaction. As a result, the product monomer **2** was obtained. The yield of the purplish product was 98% (0.92 g). ^{1}H NMR (400 MHz, $CDCl_3$) δ (ppm): 8.10 (d, 4H, $J = 8.4$ Hz), 7.68 (d, 4H, $J = 8.4$ Hz), 7.53–7.44 (m, 6H), 7.42 (d, 4H, $J = 7.5$ Hz). EA data of monomer **2** could not be obtained due to the high moisture sensitivity of acid chloride.

2.1.8. Polymerization of light-emitting polymer PTOA

A reaction mixture containing monomer **1** (0.92 g), monomer **2** (0.7883 g), 2,4,6-collidine (0.526 mL), and anisole (39.87 mL) was heated to reflux in a nitrogen atmosphere for 72 h. After cooling, the solvent was removed under vacuum. The polymer was dissolved in a small amount of chloroform and was precipitated repeatedly into methanol–water several times. The purified polymer was filtered and dried under vacuum. The yield of the yellow solid was 61% (0.88 g). The number and weight average molecular weight of the PTOA measured by GPC were about 6000 and 10,620 g/mol, respectively, with a polydispersity index of 1.77. ^{1}H NMR (400 MHz, DMSO) δ (ppm): 8.10 (d, 4H, $J = 22.4$ Hz), 7.98 (d, 4H, $J = 8.2$ Hz), 7.71 (d, 4H, $J = 18.6$ Hz), 7.57–7.53 (m, 4H), 7.47–7.39 (m, 8H), 7.20–7.16 (d, 4H, $J = 14.6$ Hz), 7.07 (d, 2H, $J = 7.5$ Hz), 2.36 (s, 3H). Anal. Calcd for $C_{47}H_{33}N_5O_2Si$: C, 75.68; H, 5.06; N, 7.97. Found: C, 77.27; H, 4.80; N, 9.59.

2.2. Instruments

^{1}H NMR spectra were recorded on a Bruker AMX-400 MHz spectrometer. The elemental analysis was carried out with elemental analyzer (Elementar Vario EL III). Gel permeation chromatography (GPC) measurements were carried out on a Waters chromatography (Waters, 717 plus Autosampler). Two Waters Styragel linear columns were used, with polystyrene as standard and THF as eluent. Glass transition temperature (T_g) was measured by differential scanning calorimetry (DSC: TA Instruments, DSC-2010) in a nitrogen atmosphere at a heating rate of 10 °C/min. Thermogravimetric analysis (TGA) of the polymer was performed in a nitrogen atmosphere at a heating rate of 10 °C/min by using a Thermogravimetric Analyzer (TA Instruments, TGA-2050). The UV–vis spectrum was measured using a Hewlett–Packard 8453 with a photodiode array detector. Photoluminescence and electroluminescence spectra were recorded on a Hitachi F-4500 fluorescence spectrophotometer. The morphology of the LEP solid films was studied using an atomic force microscope (Digital Instrument: Dimension 3100 Series Scanning Probe Microscope). Redox potentials of the polymer were determined by cyclic voltammetry (CV) using a BAS 100B electrochemical analyzer with a scanning rate at 100 mV/s.

The polymer was dissolved in deoxygenated dry DMF with 0.1 M tetrabutylammonium perchlorate as the electrolyte. A platinum working electrode and a saturated nonaqueous Ag/$AgNO_3$ referenced electrode were used. Ferrocene was used for potential calibration (all reported potentials are referenced against Ag/Ag^+) and for reversibility criteria. The fluorescence quantum yield of the LEP solid film was determined by the integrating-sphere method, described by Mello et al. on vacuum deposited thin films [47]. A He–Cd laser beam (Kimmon, He–Cd laser, 325 nm, 0.17 mW) interacts with a liquid or solid sample located inside an integrating sphere with an internal diffuse white reflectance coating. The uniformly scattered radiation is coupled to a fused silica fiber through a baffle-blocked opening, and is detected by a spectrally calibrated spectrometer CCD system.

2.3. EL device fabrication and characterization

The PLED structure in this study is ITO glass/PEDOT/PTOA–PVK/Ca/Al. ITO-coated glass, with a sheet resistance of 15 Ω/sq, was purchased from Applied Film Corp. Glass substrates with patterned ITO electrodes were well washed and cleaned by O_2 plasma treatment. A thin film (500 Å) of hole-transporting material PEDOT (AI4083, Bayer) was formed on the ITO layer of a glass substrate by the spin-casting method. The PTOA–PVK composite films in different weight ratios were then spin-coated from the 20 or 15 mg/mL of cyclohexanone solution onto the PEDOT layer, and were dried at 80 °C for 1 h in a glove box. A high-purity Ca cathode was thermally deposited onto the PTOA thin film, followed by the deposition of Al metal as the top layer, in a high-vacuum chamber. After the electrode deposition, the PLED was transferred from the evaporation chamber to a glove box purged by high-purity nitrogen gas to keep oxygen and moisture levels below 1 ppm. The device was then encapsulated by glass covers, which was sealed with UV-cured epoxy glue in the glove box. The deposition rate of cathode was determined with a quartz thickness monitor (STM-100/MF, Sycon). The thickness of the thin film was determined with a surface texture analysis system (3030ST, Dektak). Current–voltage characteristics were measured on a programmable electrometer with current and voltage sources (Keithley 2400). Luminance was measured with a BM-8 luminance meter (Topcon).

3. Results and discussion

3.1. Synthesis and thermal properties of PTOA

The triarylaminooxadiazole-containing tetraphenylsilane light-emitting polymer, PTOA, was obtained using a modified Huisgen reaction. The chemical structure of the PTOA was confirmed by ^{1}H NMR spectroscopy and elemental analysis. Fig. 1 shows the ^{1}H NMR spectra of the PTOA. The chemical shifts and the relative intensities of the signals are in agreement with the proposed structures for the PTOA. PTOA is readily soluble in common organic solvent, such as THF, toluene, and cyclohexanone. The thermal properties of the PTOA were analyzed using DSC and TGA in a nitrogen atmosphere. The thermal stability of LEP plays an important role on the operating stability of PLEDs. The operational lifetime of the PLED is directly related to the T_g and the thermal stability of the LEP [28]. High T_g and T_d are favorable for the application of LEPs in the outdoor display. The DSC result shows that PTOA possesses a very high T_g of 218 °C. The 5% weight loss degradation temperature appeared at 373 °C. This tetraphenylsilane-based LEP shows excellent thermal stability compared

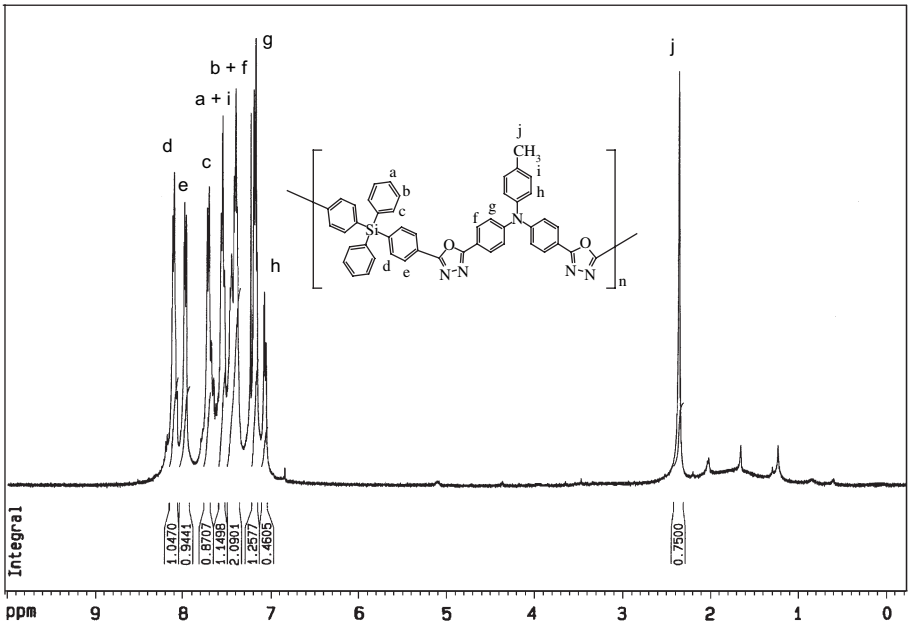

Fig. 1. ^{1}H NMR spectrum of the light-emitting polymer.

to that of the soluble LEPs, such as poly(phenylene vinylene) [48] or polyalkylfluorenes [49]. The incorporation of the rigid moieties of the tetraphenylsilane and arylamino groups into the polymer backbone considerably reduces the molecular mobility of the polymer main chain, thus increasing the T_g of the LEP.

3.2. Morphology study of PTOA-based solid film

The morphology of the PTOA solid films after being annealed at elevated temperatures has been investigated using AFM microscopy. Figs. 2 and 3 show the AFM micrographs of the PTOA film after thermal treatment at 200 °C, 230 °C, and 250 °C for 5 h. In Fig. 2, the phase image and topography indicate that the PTOA solid film remains in an amorphous state after being thermally treated at 200 °C for 5 h. As the polymer film is annealed at a higher temperature of 230 °C, the polymer chain gains high mobility, altering the chain conformation, and leading to aggregate formation and isolated crystalline domains. This is called cold crystalline or accessory crystalline [50]. In Fig. 3, the phase image clearly indicated that the snail shell-like isolated crystal was formed due to the thermal annealing of the PTOA film at a temperature much higher than T_g. The topographic 3D view shows that the height of the snail shell-like isolated crystal was about 23.5 nm. The diameter of the crystal was about 105 nm. It is concluded that the AFM image is the evidence of the morphological change of the PTOA solid film after being annealed at temperature above T_g.

3.3. Optical properties of PTOA

The UV–vis absorption and the PL spectra of the PTOA in diluted solution and in solid-film state are shown in Fig. 4. The PTOA in solution has two absorption bands at 300 nm and 375 nm. The absorption band at 300 nm attributes to the oxadiazole unit [51]. The main peak at 375 nm is accompanied by a shoulder at approximately 335 nm. The absorption band with a 375 nm maximum attributes to the π-conjugation between diphenyl(*para*-tolyl)amine and the oxadiazole unit. The shoulder near 335 nm originates from diphenyl(*para*-tolyl)amine absorption [21]. The PTOA film maximum absorption observed at 380 nm is slightly red-shifted compared to PTOA in solution. In solution, PTOA shows photoluminescence (PL)

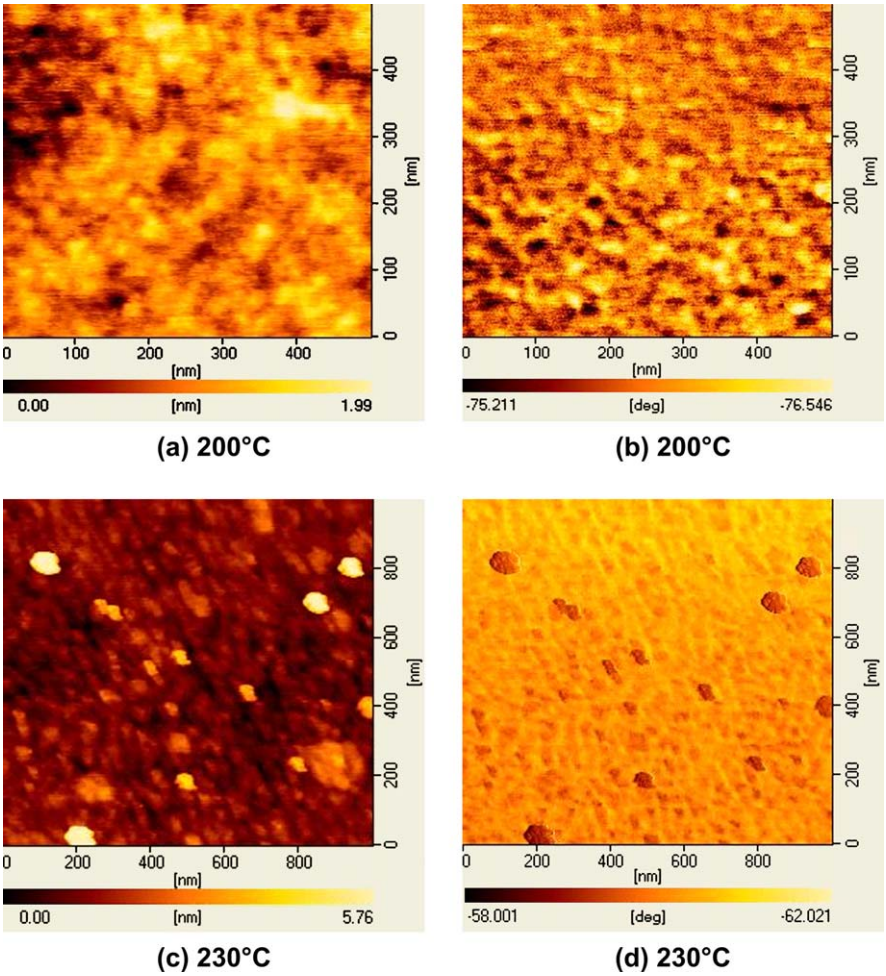

Fig. 2. AFM spectra of PTOA-based solid film after thermal annealing at 200 °C and 230 °C for 5 h ((a) and (c): topography image; (b) and (d): phase image).

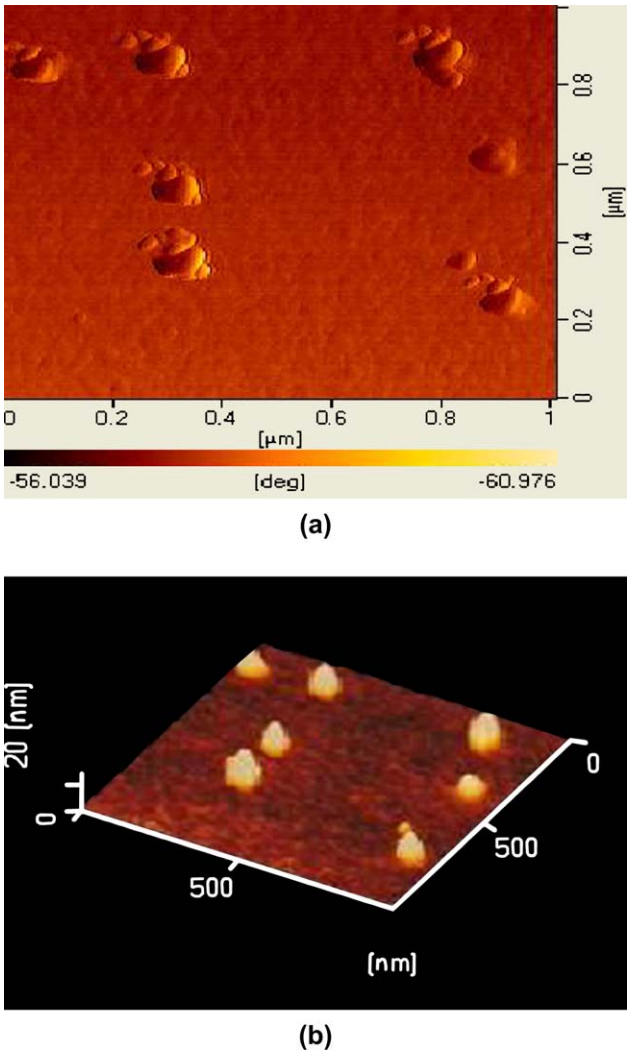

Fig. 3. AFM spectra of PTOA-based solid film after thermal annealing at 250 °C for 5 h ((a): phase image; (b): topography 3D image).

with emission maxima at 426 nm, which is attributed to the light-emitting unit of the triarylaminooxadiazole group. In solid film the emission maximum of PL was observed at 458 nm, which has a 32 nm red-shift from the PL in solution. The solvatochromic effect and excimer (or exciplex) formed in the solid film are responsible for the red-shift and broadening of the PL emission band. The excimer (M*M) and exciplex (M*N) are attributed to the interaction between the oxadiazole (M) groups, and the oxadiazole and diphenyl(4-tolyl)amine groups (N) in different polymer segments or chains, respectively [52,53]. The PL quenching of excimer and exciplex results in the lower fluorescence quantum yield (1.38%) of the PTOA solid film.

The PL stability and morphology of the PTOA solid film were further investigated by thermal annealing at elevated temperatures. Fig. 5 shows the normalized PL spectra of PTOA solid films after being heat treated at 200 °C, 230 °C, and 250 °C for 5 h. No significant difference of PL spectra and morphological change was observed between pristine samples and repeatedly thermally annealed film (at 200 °C). The polymer chain was frozen and maintained the existing morphology as the annealed temperature was below glass transition. As a result the PL spectrum of the solid film was not changed after being heat treated at 200 °C for 5 h. After the solid films were annealed at 230 °C or 250 °C for 5 h the shape of the maximum PL emission peak at 458 nm was only slightly different compared to a pristine sample. However, a weak shoulder emission peak was observed at around 620 nm for solid film heat treated at 230 °C. Furthermore, a shoulder emission peak appeared at around 550 nm when increasing the annealing temperature to 250 °C. This implies that the morphology of the polymer solid film was modified after being annealed at temperatures above T_g. An aggregation or excimer (and exciplex) was formed among the polymer chains, which lead to the occurrence of an inter-chain exciton emission at a longer wavelength. A similar phenomenon has been observed in the thermal treatment of MEH–PPV film,

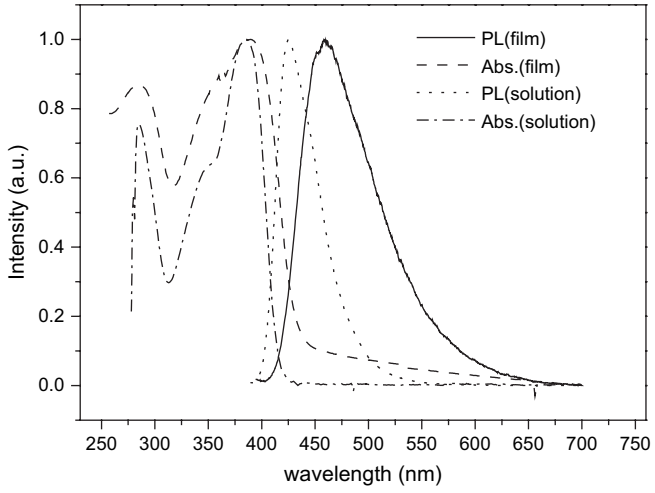

Fig. 4. UV–vis absorption and PL spectra of light-emitting polymer in cyclohexanone solution and thin solid film (exciting wavelength of PL: 390 nm).

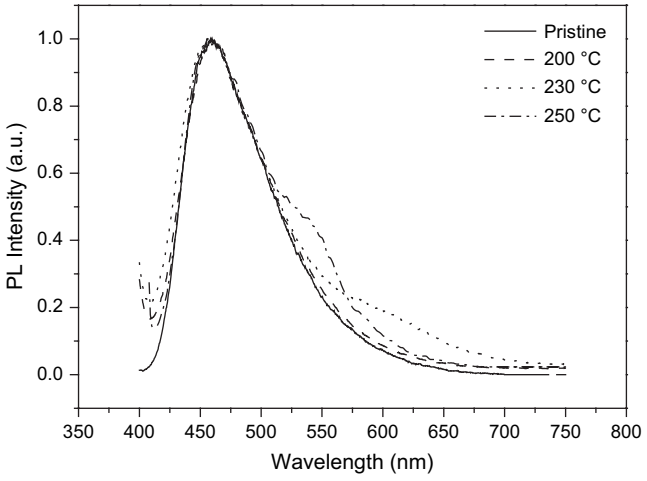

Fig. 5. PL spectra of PTOA solid film after being heat treated at elevated temperature for various times (heating at 200 °C, 230 °C, and 250 °C for 5 h).

which has been reported by Liu et al. [54]. After the solid film anneals at 230 °C the polymer chain gains some mobility, resulting in the aggregation or excimer (and exciplex) formation of polymer chains. Consequently, inter-chain exciton emission at 620 nm was obtained. Furthermore, polymer chain mobility is enhanced when thermal treatment temperature increased to 250 °C. High thermal energy causes chain conformation change to a higher inter-chain order or packing density. In other words, a shorter or localized conjugation length in the snail shell-like isolated crystal results in a blue-shift of inter-chain exciton emission wavelength from 620 nm to 550 nm.

3.4. Electrochemical properties of PTOA

Cyclic voltammetry was employed to investigate the electrochemical behavior, and to estimate the highest occupied molecular orbital (HOMO) and the lowest unoccupied (LUMO) energy levels of PTOA. Fig. 6 shows the cyclic voltammograms of PTOA. The potentials of oxidation and reduction were observed at 0.64 eV and −2.04 eV, respectively. The oxidation and reduction would selectively start at the hole- and electron-transporting segments (diphenyl(4-tolyl)amine and oxadiazole units), respectively. The HOMO energy level of PTOA was calculated from the onset potential of oxidation by assuming the absolute energy level of ferrocene is 4.8 eV below the vacuum level, and the LUMO energy level was calculated from the HOMO energy level and the absorption edge [55,56]. The onset potential of oxidation (E^{ox}_{onset}) was about 0.49 eV. Moreover, the optical band gap (E_g) of the PTOA, determined from the absorption edge, was 2.86 eV. The electron affinity (LUMO level) and ionization potential (HOMO level) of the PTOA were 2.45 eV and 5.3 eV, respectively. In comparison with the work function of the cathodic material, e.g., Ca/Al (2.9 eV), a small electron injection barrier exists for PTOA. On the other hand, the HOMO energy level is 5.3 eV, so no hole injection barrier to the anodic material (e.g., ITO (5.2 eV)) exists.

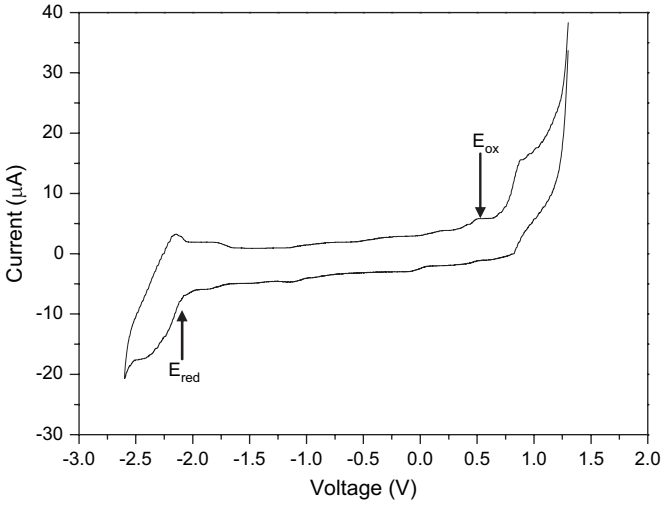

Fig. 6. Cyclic voltammograms of light-emitting polymer PTOA.

3.5. Electroluminescence properties of PTOA-based PLEDs

The electroluminescence (EL) spectra of the PTOA-based PLED (device I) at various applied voltages are shown in Fig. 7. Device I exhibits EL with a main peak at 458 nm accompanied by a shoulder at around 530 nm. The light emission from electromer $(M^+M^-)^*$ or electroplex $(M^+N^-)^*$ leads to the broadening of the EL spectra (400–650 nm), which corresponds to the interaction between the oxadiazole (M) and diphenyl(4-tolyl)amine (N) groups in different polymer segments or chains [53,54]. However, the amplitude of the electric field-induced electromer or electroplex was not pronounced for the device I. The EL band or color purity (CIE(0.19,0.22)–CIE(0.22,0.25)) did not change significantly with increasing applied voltage. A sky blue emission was obtained for device I. The electroluminescence properties of device I are shown in Fig. 8. The brightness and efficiency of the PLEDs can be as high as 248 cd/m^2 and 0.54 cd/A, respectively. The brightness and efficiency of PTOA-based

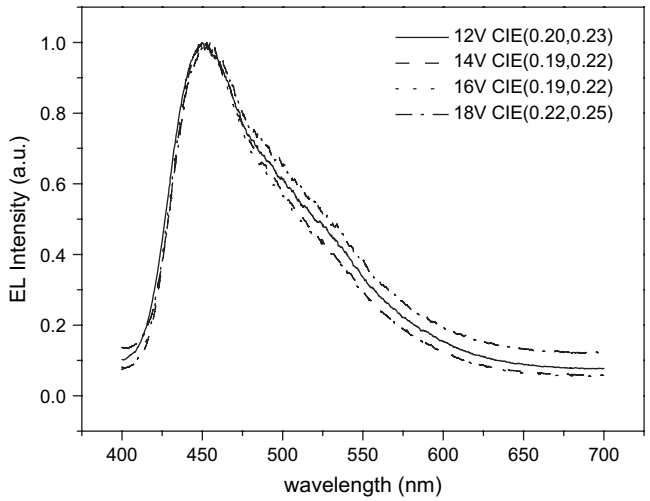

Fig. 7. EL spectra of PTOA-based PLED (device I: ITO/PEDOT (50 nm)/PTOA (84 nm)/Ca (15 nm)/Al (120 nm)) at various applied voltages.

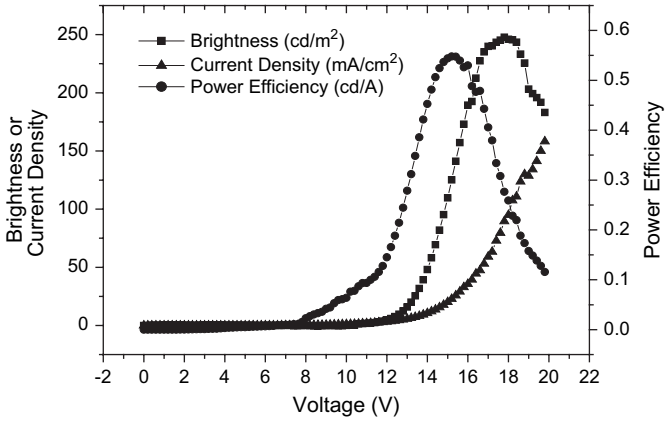

Fig. 8. Electroluminescence properties of PTOA-based PLED (device I: ITO/PEDOT (50 nm)/PTOA (84 nm)/Ca (15 nm)/Al (120 nm)).

PLED were not as high as we expected due to the EL quenching of electromer or electroplex. The formation of electromer or electroplex between the oxadiazole and diphenyl(4-tolyl)-amine was not observed for the small molecular weight compound of (4-(5(4-(diphenylamino)phenyl)-2-oxadiazolyl)-phenyl)triphenylsilane (Ph_3Si(PhTPAOXD)) [19]. This may be due to the fact that the interaction between the oxadiazole and the diphenyl(4-tolyl)amine of the two molecules was resisted by the steric hindrance of tetraphenylsilane. However, the morphology of the light-emitting polymer PTOA was not the same as the Ph_3Si(PhTPAOXD) based thin film. The conformation of the polymer chains is affected by the thin-film processing conditions, such as the kind of organic solvent, the concentration of polymer solution, and the spin-rate during the spin-coating process [6]. This allows the opportunity for contact between the two oxadiazole groups, and oxadiazole and diphenyl(4-tolyl)amine groups, among the different polymer segments, leading to the formation of electromer or electroplex and EL quenching of PTOA-based device.

3.6. PL and EL properties of the PTOA–PVK-based PLEDs

In order to reduce the excimer and exciplex between the different polymer segments the PTOA was blended with PVK in different weight ratios. The PL spectra of the PTOA–PVK composite-based solid films are shown in Fig. 9. The composition, film thickness, wavelength of emission maximum of PL, full width at half-maximum (FWHM) of PL, and fluorescence quantum efficiency (ϕ_f) of the PTOA–PVK composite films are summarized in Table 1. In Fig. 9, PVK shows a broad emission band with the maximum at about 395 nm. PTOA–PVK-based solid film shows PL with a main peak at 458 nm accompanied by a shoulder at about 350–400 nm. The shoulder peak was attributed to the oxadiazole, which is excited at 300 nm. Moreover, PL emission from PVK was absorbed completely by the triarylaminooxadiazole group of PTOA *via the Forster-type energy transfer* process for the PTOA–PVK composite film. The emission maximum of PL was blue-shifted and FWHM became narrower with increasing PVK content, which corresponds to the reduction of excimer or exciplex between the oxadiazole and diphenyl(4-tolyl)amine in different polymer segments. The ϕ_f of the solid film was also enhanced with increasing PVK content because of the reduction of the excimer and exciplex effects. The maximum of ϕ_f (10.0%) was obtained for the PTOA–PVK film containing 50 wt.% of PVK. In addition, the EL spectra of the PTOA-based device (device II) at various applied voltages are shown in Fig. 10(a). The emission intensity from electromer or electroplex increased with increasing applied voltage for device II, especially when the voltage was increased up to 18 V. This demonstrated that the electron-donor and electron-acceptor of diphenyl(4-tolyl)amine and oxadiazole in different polymer segments tended to attract one another in the applied high electric field. However, the electric field effect on the formation of electromer or electroplex was not observed clearly in device I. This is due to the fact that the light-emitting layer of device I was thicker than device II. The intensity of the electric field through the light-emitting layer of device I was lower in comparison with device II. As a result, the emission band from electromer or electroplex was more pronounced for device II compared to that of device I. In addition, the EL spectra of the PTOA–PVK composite film-based PLEDs (devices II–VI) are shown in Fig. 10(b). The emission maximum of EL was blue-shifted and FWHM became narrower with increasing PVK content due to the reduction of aggregation by dilution effect of PVK. The wavelength of emission maximum of EL, FWHM of EL, and CIE coordinates of the PTOA–PVK composite film-based devices are

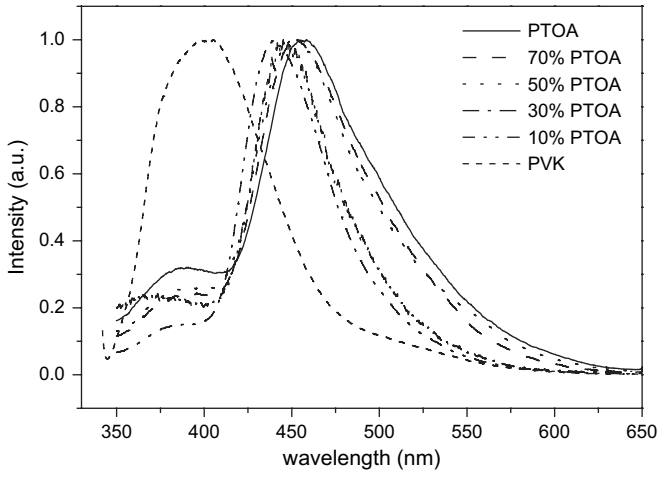

Fig. 9. PL spectra of PTOA and PVK based composite films (exciting wavelength: 300 nm).

Table 1
The film thickness, PL, and EL properties of PTOA–PVK composite film-based devices

Device no.	PTOA–PVK (wt.%)	d (nm)	λ_{max}^{PL} (nm)	FWHM of PL (nm)	λ_{max}^{EL} (nm)	FWHM of EL at 18 V	CIE (x,y) at 18 V	ϕ_f (%)	Maximum luminance (cd/m^2)	Maximum efficiency (cd/A)
I	100/0	84	457	83	458	99	(0.20,0.26)	7.7	248	0.54
II	100/0	71	453	81	454	120	(0.19,0.26)	7.1	583	0.36
III	70/30	73	451	76	450	84	(0.18,0.20)	8.9	485	0.69
IV	50/50	76	450	75	444	58	(0.17,0.14)	10.0	326	0.83
V	30/70	81	447	56	439	57	(0.16,0.10)	9.1	503	0.41
VI	10/90	86	440	57	434	49	(0.16,0.07)	8.9	102	0.23

d: Thickness of light-emitting layer; FWHM: full width at half-maximum; ϕ_f: fluorescence quantum efficiency of solid film.

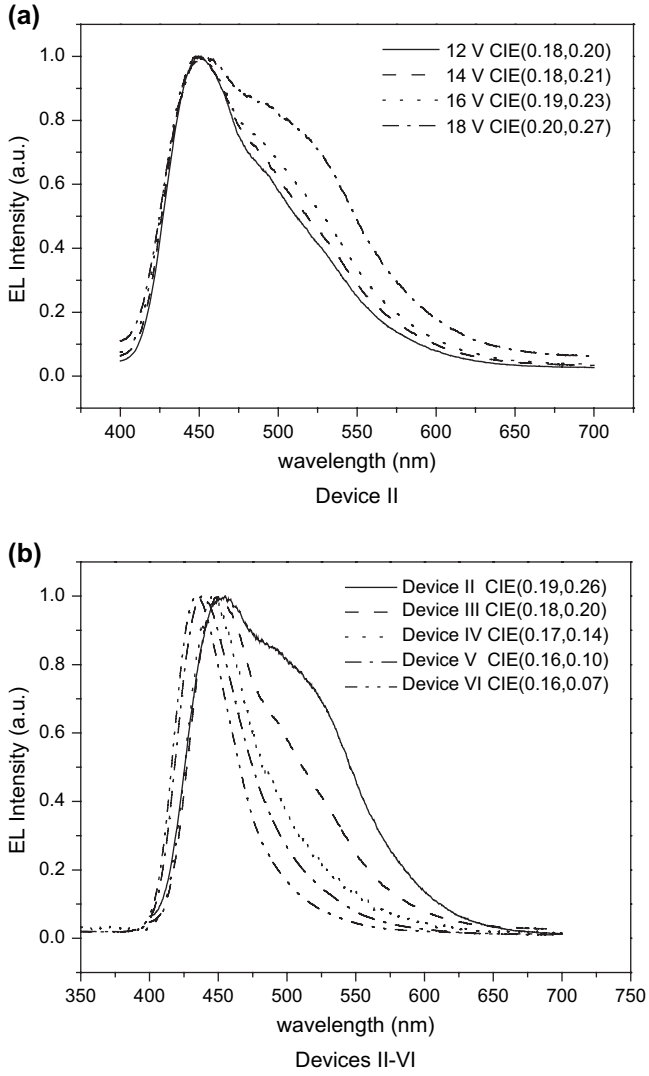

Fig. 10. EL spectra of PTOA–PVK composite film-based PLEDs: (a) device II under different applied voltages (12–18 V) and (b) devices II–VI under applied voltage of 18 V; devices II–VI: ITO/PEDOT (50 nm)/PTOA–PVK (X nm)/Ca (15 nm)/Al (120 nm).

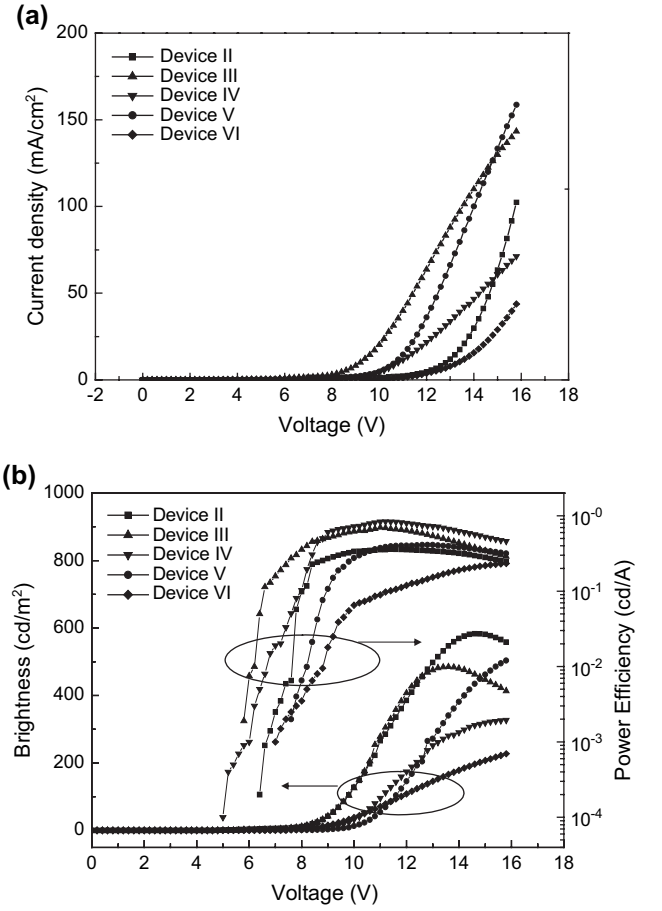

Fig. 11. Electroluminescence properties of PTOA–PVK composite film-based PLEDs (devices II–VI: ITO/PEDOT (50 nm)/PTOA–PVK (*X* nm)/Ca (15 nm)/Al (120 nm) under different applied voltage.

summarized in Table 1. The color purity of the blue emission band was enhanced with increasing PVK content. High color purity of blue emission with CIE (0.16,0.07) was obtained for the device VI.

The electroluminescence properties of the PTOA–PVK composite-based devices are shown in Fig. 11. A higher brightness and current density were observed for device II in comparison with the device I. For PLED with a thin light-emitting layer, polymer chains extended more thoroughly due to spin-coating process with high spin-rate [4]. This is favorable for carrier transport and recombination. Therefore, device II obtained high brightness and current density [4]. Higher brightness and current density in device II was partially due to its thinner thickness compared to device I. Furthermore, the roughness of the ITO surface could not be smoothed down by a thin polymer film. As a result, electric leakage could have occurred during the operation processes of the PLED because of the presence of defects. Consequently, low power efficiency was obtained for device II. For the devices II–IV, the incorporation of PVK into PTOA not only affects the brightness but the power efficiency of the PLED as well. Current density and brightness decreased with increasing PVK content partially due to LEP enhanced thickness. Thicker light-emitting films with lower electric fields obtained lower current density and brightness. Reduced PTOA content also contributed to reduced current density and brightness. On the other hand, the power efficiency increased with increasing PVK content. This is because of the reduction of electromer or electroplex effects and the reduction in the number of defects on the anode surface. For device V, the highest brightness was obtained owing to the fact that the electromer or electroplex effects diminished completely as the PVK content increased up to 70 wt.%. However, the excess content of PVK was not favorable for the enhancement of the power efficiency of the PLED. The brightness and power efficiency decreased rapidly with further increasing of the PVK content. The maximum of the brightness and power efficiency is also summarized in Table 1. Results indicate that EL performance of PLEDs strongly depends on light-emitting layer of the PVK content.

3.7. Thermal stability of EL performance of PTOA–PVK solid film-based device

In order to study the thermal stability of EL performance, the PTOA–PVK solid film-based device has been annealed at elevated temperatures for various times. Fig. 12 shows the EL spectra of device V after being annealed at 150 °C for 2 h and 4 h. The emission band did not change after being thermally treated, which implies that the microstructure or morphology of the PTOA–PVK composite film was stable at elevated temperatures. However, the current density and brightness of device V decayed rapidly after being thermally treated (as shown in Fig. 13). The power efficiency was not affected by the thermal treatment. The reduction of brightness implies that the light-emitting layer was degraded and the device was damaged by applying a high electric field. The degradation of the light-emitting layer was attributed to the electrically induced degradation of the oxadiazole moiety. However, the PTOA–PVK composite film-based device shows excellent EL spectrum stability at elevated temperatures.

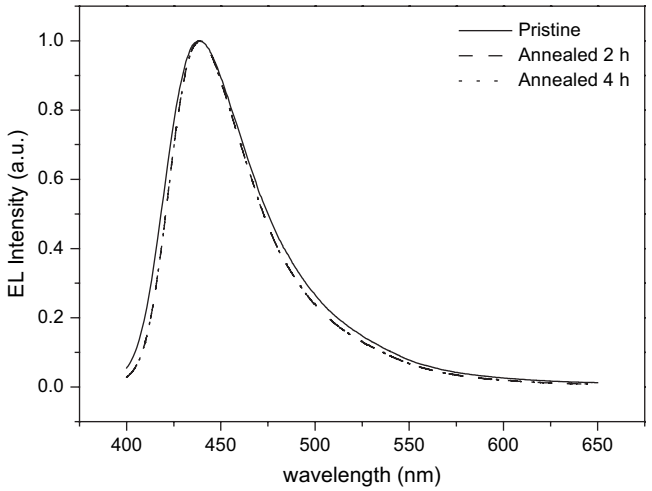

Fig. 12. EL spectra of device V after being thermally annealed at 150 °C for various times.

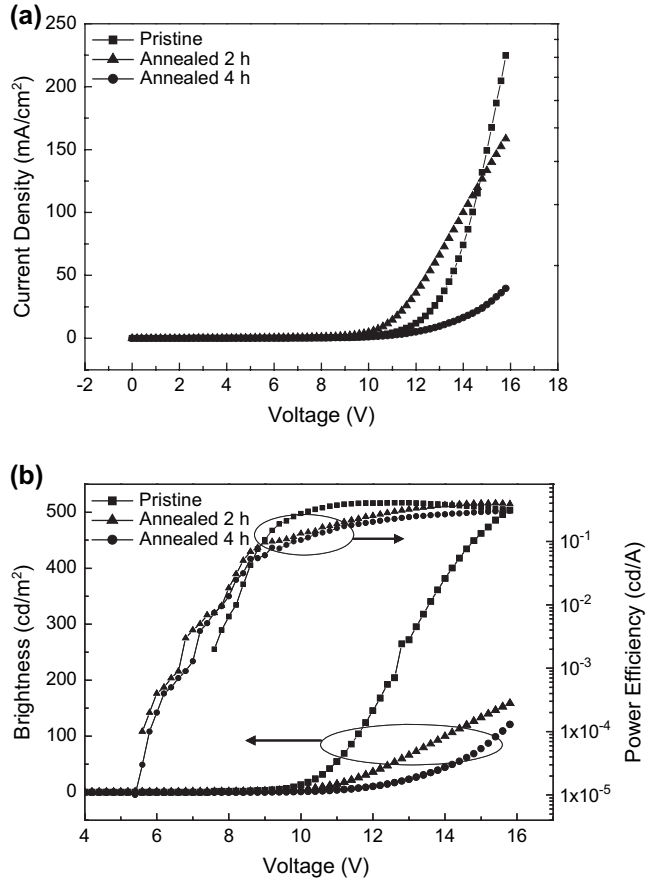

Fig. 13. Electroluminescence property of device V after being thermally annealed at 150 °C for 2 h and 4 h.

4. Conclusion

A novel triarylaminooxadiazole-containing tetraphenylsilane light-emitting polymer (PTOA) has been synthesized. Excellent thermal stability was observed due to the presence of a rigid tetraphenylsilane-based polymer backbone. The light emission from electromer and electroplex leads to a broadening of the EL spectra, which corresponds to the interaction between the oxadiazole and diphenyl(4-tolyl)amine groups in different polymer segments or chains. Furthermore, the emission intensity from electromer and electroplex was enhanced by the electric field. The brightness and efficiency of PTOA-based PLED were moderate due to the EL quenching of electromer and electroplex effects. The electromer and electroplex could be diminished completely by the incorporation of PVK in the PTOA film. As a result, the EL performance of PTOA-based PLED was improved. Higher brightness, greater power efficiency, and high color purity of blue emission with CIE (0.16,0.07) were obtained for the PTOA–PVK composite single layer device.

Acknowledgments

The authors thank the National Science Council of Taiwan, ROC, for financial support (Grant NSC93-2218-E-224-003). Helpful assistance in the measurements of AFM from Prof. J.J. Lin is also acknowledged.

References

[1] Kobayashi H, Kanbe S, Seki S, Kigchi H, Kimura M, Yudasaka I, et al. Synth Met 2000;111–112:125–8.
[2] Vaart NCVD, Lifka H, Budzelaar FPM, Rubingh JEJM, Hoppenbrouwers JJL, Dijksman JF, et al. SID Symp 2004;35:1284–7.
[3] Liu J, Shi Y, Ma L, Yang Y. J Appl Phys 2000;88:605–9.
[4] Shi Y, Liu J, Yang Y. J Appl Phys 2000;87:4254–63.
[5] Fletcher RB, Lidzey DG, Bradley DDC, Walker S, Inbasekaran M, Woo EP. Synth Met 2000;111–112:151–3.
[6] Lee RH, Lee YZ, Chao CI. J Appl Polym Sci 2006;100:133–41.
[7] Kulkarni AP, Tonzola CJ, Babel A, Jenekhe SA. Chem Mater 2004;16:4556–73.
[8] Chen ZK, Meng H, Lai YH, Huang W. Macromolecules 1999;32:4351–8.
[9] Chung SJ, Kwon KY, Lee SW, Jin JI, Lee CH, Lee CH, et al. Adv Mater 1998;10:1112–6.

[10] Lee NHS, Chen ZK, Chua SJ, Lai YH, Huang W. Thin Solid Films 2000; 363:106–9.
[11] Wu FI, Reddy DS, Shu CF. Chem Mater 2003;15:269–74.
[12] Kim JH, Lee H. Synth Met 2004;144:169–76.
[13] Chen SH, Chen Y. Macromolecules 2005;38:53–60.
[14] Tamoto N, Adachi C, Nagai K. Chem Mater 1997;9:1077–85.
[15] Thomas KRJ, Lin JT, Tao YT, Chuen CH. Chem Mater 2004;16: 5437–44.
[16] Lee YZ, Chen SA. Synth Met 1999;105:185–90.
[17] Chan LH, Yeh HC, Chen CT. Adv Mater 2001;13:1637–41.
[18] Yeh HC, Lee RH, Chan LH, Lin TYJ, Chen CT, Balasubramaniam E, et al. Chem Mater 2001;13:2788–96.
[19] Chan LH, Lee RH, Yeh HC, Chen CT. J Am Chem Soc 2002;124: 6469–79.
[20] Lee RH, Yeh HC, Chan LH, Chen CT. Synth Met 2003;137:1035–6.
[21] Ha J, Vacha M, Khanchaitit P, Ong DA, Lee SH, Ogio K, et al. Synth Met 2004;144:151–8.
[22] Liao L, Pang Y, Ding L, Karasz FE. Macromolecules 2004;37:3970–2.
[23] Lee YZ, Chen X, Chen SA, Wei PK, Fann WS. J Am Chem Soc 2001; 123:2296–307.
[24] Patra A, Pan M, Friend CS, Lin TC, Cartwright AN, Prasad PN, et al. Chem Mater 2002;14:4044–8.
[25] Pudzich R, Salbeck J. Synth Met 2003;138:21–31.
[26] Niu YH, Chen B, Liu S, Yip H, Bardecker J, Jen AKY, et al. App Phys Lett 2004;85:1619–21.
[27] Pu YJ, Kurata T, Soma M, Kido J, Nishide H. Synth Met 2004;143: 207–14.
[28] Kreyenschmidt M, Klaerner G, Fuhrer T, Ashenhurst J, Karg S, Chen WD, et al. Macromolecules 1998;31:1099–103.
[29] Becker S, Ego C, Grimsdale AC, List EJW, Marsitzky D, Pogantsch A, et al. Synth Met 2002;125:73–80.
[30] Ego C, Grimsdale AC, Uckert F, Yu G, Srdanov G, Mullen K. Adv Mater 2002;14:809–11.
[31] Li H, Hu Y, Zhang Y, Ma D, Wang L, Jing X, et al. Chem Mater 2002;14: 4484–6.
[32] Liu XM, He C, Hao XT, Tan LW, Li Y, Ong KS. Macromolecules 2004; 37:5965–70.
[33] Kim IU, Lee HB, Shin JS, Kim YH, Joe YK, Oh HY, et al. Synth Met 2005;150:27–32.
[34] Huser T, Yan M. Synth Met 2001;116:333–7.
[35] Lee TW, Park OO. Adv Mater 2000;12:801–4.
[36] Collison CJ, Rothberg LJ, Treemaneekarn V, Li Y. Macromolecules 2001;34:2346–52.
[37] Chen SH, Su AC, Han SR, Chen SA, Lee YZ. Macromolecules 2004;37: 181–6.
[38] Sung HH, Lin HC. Macromolecules 2004;37:7945–54.
[39] Grimsdale AC, Leclere P, Lazzaroni R, Mackenzie JD, Murphy C, Setayesh S, et al. Adv Funct Mater 2002;12:729–33.
[40] Jacob J, Zhang J, Grimsdale AC, Mullen K, Gaal M, List EJW. Macromolecules 2003;36:8240–5.
[41] Zeng G, Yu WL, Chua SJ, Huang W. Macromolecules 2002;35:6907–14.
[42] Palilis LC, Lidzey DG, Redecker M, Bradley DDC, Inbasekaran M, Woo EP, et al. Synth Met 2000;111–112:159–63.
[43] Sainova D, Miteva T, Nothofer HG, Scherf U, Glowacki I, Ulanski J, et al. Appl Phys Lett 2000;76:1810–2.
[44] He G, Liu J, Li Y, Yang Y. Appl Phys Lett 2002;80:1891–3.
[45] Nishiyama M, Yamamoto T, Koie Y. Tetrahedron Lett 1998;39:617–20.
[46] Yamamoto T, Nishiyama M, Koie Y. Tetrahedron Lett 1998;39:2367–70.
[47] Mello JCD, Wittmann HF, Friend RH. Adv Mater 1997;9:230–3.
[48] Mikroyannidis JA, Spiliopoulos IK, Kasimis TS, Kulkarni AP, Jenekhe SA. Macromolecules 2003;36:9295–302.
[49] Zheng L, Urian RC, Liu Y, Jen AKY. Chem Mater 2000;12:13–5.
[50] Niu YH, Hou Q, Cao Y. Appl Phys Lett 2002;81:634–6.
[51] Tsutsui T, Aminaka EI, Tokuhisa H. Synth Met 1997;85:1201–4.
[52] Lee YZ, Chen X, Chen MC, Chen SA. Appl Phys Lett 2001;79:308–10.
[53] Giro G, Cocchi M, Kalinowski J, Marco PD, Fattori V. Chem Phys Lett 2000;318:137–41.
[54] Liu J, Guo TF, Yang Y. J Appl Phys 2002;91:1595–600.
[55] Miller LL, Nordblom GD, Mayeda EA. J Org Chem 1972;37:916–8.
[56] Yang CJ, Jenekhe SA. Macromolecules 1995;28:1180–96.